

ReACT-TTC: Capacity-Aware Top Trading Cycles for Post-Choice Reassignment in Shared CPS

Anurag Satpathy*

anurag.satpathy@mst.edu

Department of Computer Science

Missouri University of Science and Technology

Rolla, MO, USA

Chittaranjan Swain

cswain@iitm.ac.in

Indian Institute of Information Technology and

Management Gwalior

Gwalior, Madhya Pradesh, India

Arindam Khanda*

akkcm@mst.edu

Department of Computer Science

Missouri University of Science and Technology

Rolla, MO, USA

Sajal K. Das

sdas@mst.edu

Department of Computer Science

Missouri University of Science and Technology

Rolla, MO, USA

Abstract

Cyber-physical systems (CPS) increasingly manage shared physical resources in the presence of human decision-making, where system-assigned actions must be executed by users or agents in the physical world. A fundamental challenge in such settings is user non-compliance: individuals may deviate from assigned resources due to personal preferences or local information, degrading system efficiency and requiring light-weight reassignment schemes. This paper proposes a post-deviation reassignment framework for shared-resource CPS that operates on top of any initial allocation algorithm and is invoked only when users diverge from prescribed assignments. We advance the Top-Trading-Cycle (TTC) mechanism to enable voluntary, preference-driven exchanges after deviation events, and extend it to handle many-to-one resource capacities and unassigned resource conditions that are not supported by the classical TTC. We formalize these structural cases, introduce capacity-aware cycle-detection rules, and prove termination along with the preservation of Pareto efficiency, individual rationality, and strategy-proofness. A Prospect-Theoretic (PT) preference model is further incorporated to capture realistic user satisfaction behavior. We demonstrate the applicability of this framework on an electric-vehicle (EV) charging case study using real-world data, where it increases user satisfaction and effective assignment quality under non-compliant behavior.

Keywords

Cyber-physical systems, Human-in-the-loop, Resource allocation, Top trading cycles, Non-compliant users, Electric vehicle charging.

*The authors contributed equally to this work.

This is a preprint of a paper accepted in 17th ACM/IEEE International Conference on Cyber-Physical Systems (ICCPs), Saint Malo, France, May 11-14, 2026.

Permission to make digital or hard copies of all or part of this work for personal or classroom use is granted without fee provided that copies are not made or distributed for profit or commercial advantage and that copies bear this notice and the full citation on the first page. Copyrights for third-party components of this work must be honored. For all other uses, contact the owner/author(s).

ICCPs '26, St. Malo, France

© 2026 Copyright held by the owner/author(s).

ACM ISBN 978-x-xxxx-xxxx-x/YYY/MM

<https://doi.org/10.1145/nnnnnnnn.nnnnnnnn>

1 Introduction

Cyber-Physical Systems (CPS) increasingly manage shared physical resources in large-scale, interactive environments such as mobility services [12, 42], electric vehicle charging [10, 33], smart grids [14], shared micromobility [38], autonomous parking [11], and urban logistics [32]. In these systems, a digital controller computes resource allocations or schedules, while physical agents (e.g., vehicles, drones) execute decisions in the environment. In this context, effective operation requires efficient allocation of limited resources, rapid adaptation to changing conditions, and mechanisms that account for human behavior and heterogeneous user preferences.

A key challenge in CPS environments is user *non-compliance* [46]. Even when a controller assigns routes, schedules, or resources, users often deviate based on personal convenience or local observations such as queue length, travel distance, or price [13, 22]. For example, in the EV charging scenario in Fig. 1, EV e_2 was recommended to charge at C_3 , but the user ignores it, prompting a real-time reassignment to C_4 . Such behavior is widespread: 30–60% of drivers override navigation recommendations [15, 31, 54]; 20–40% of ride-hailing users reject assigned trips [6, 49]; shared micromobility users switch parking spots when docks appear full [20]; 15–35% of drivers ignore parking guidance when walking time increases [26]; 25–50% of EV drivers divert from recommended chargers due to pricing or queues [5, 43]; 20–40% of households disregard load-shifting instructions in demand-response programs [50]; and logistics drivers routinely re-sequence deliveries [21]. These deviations violate allocation assumptions, reduce system-wide efficiency, and introduce compounding congestion or imbalance, underscoring the need for CPS mechanisms that explicitly model human decision-making and support real-time reassignment, and maintain user satisfaction.

Existing CPS coordination frameworks, including market-based scheduling [44], heuristic dispatch [25], and game-theoretic matching [2], largely assume that agents comply with assigned resources or routes. When deviations occur, most systems either ignore them or rely on centralized re-optimization, which is computationally expensive and disrupts already-committed allocations. Moreover, classical exchange-based mechanisms, such as classical Top-trading cycle (TTC) [41] and barter-style assignment [45], assume one-to-one ownership and do not naturally extend to CPS settings where (i) resources have capacity, (ii) multiple agents may share a resource,

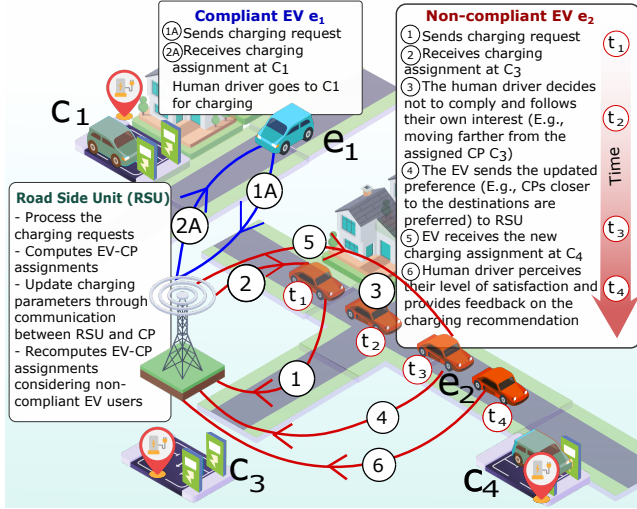


Figure 1: An electric vehicle (EV) to charging point (CP) assignment scenario with compliance and non-compliance.

and (iii) unused capacity may exist. These structural differences preclude direct use of exchange mechanisms and constrain real-time, user-aware adaptation to non-compliance.

To address these limitations, we propose a post-deviation reassignment layer that operates above existing CPS allocation mechanisms. When users deviate from assigned resources, our framework enables voluntary reassignment via a modified Top Trading Cycle (TTC) process that handles capacity-constrained and partially allocated resources, maintaining/improving user satisfaction [16]. Unlike classical TTC, which assumes one-to-one ownership, CPS settings involve shared resources (co-ownerships), quotas, and idle capacity (no-ownership). We formally characterize the structural cases arising from capacity-constrained CPS resources (shared, under-filled, and idle slots), develop resource trading procedures, and prove that the adapted TTC mechanism preserves Pareto efficiency, individual rationality, and strategy-proofness in each case. Although broadly applicable to shared-resource CPS settings, we demonstrate its effectiveness in EV charging as a representative case. This work makes the following key **contributions**:

- We propose a post-deviation reassignment layer for shared-resource CPS that augments any base allocation algorithm and activates only when users deviate.
- We develop a capacity-aware extension of TTC to enable voluntary, preference-driven exchanges in many-to-one settings with unassigned capacity.
- We identify structural cases in CPS resources (multi-user allocations and idle capacity) and derive resource-exchange rules to ensure the validity of trades and maximize user satisfaction.
- We prove termination and show that Pareto efficiency, individual rationality, and strategy-proofness are preserved under different cases.
- We incorporate a Prospect-Theoretic satisfaction model to more accurately capture human preference behavior compared to linear scoring.

- We evaluate the framework on real-world EV charging traces, demonstrating at least 43% improvement in user satisfaction and efficient reassignment under non-compliance with minimal computation overhead.

The remainder of the paper is organized as follows. Section 2 reviews related work on non-compliant CPS systems. Section 3 presents the system model and problem formulation, while Section 4 details the assignment problem and proposed solution. Theoretical analysis is provided in Section 5, followed by experimental validation in Section 6. Section 7 discusses limitations and future directions, and Section 8 concludes the paper.

2 Literature Review

Prior work spans four areas: non-compliance in CPS, dynamic resource allocation, market design mechanisms, and EV charging systems, collectively addressing bounded rationality, centralized compliance, and shared resource coordination.

2.1 Non-compliant Behavior in CPS

Studies on route-choice behavior show that compliance depends not only on system accuracy but also on how guidance is framed. In [31], drivers followed recommendations framed for collective efficiency but ignored those emphasizing personal optimization or providing excessive detail. Similarly, social-navigation experiments in [15] found that transparency and well-designed incentives improve adherence, while poor framing or low trust induces deviation.

Similar patterns appear across CPS domains. In ride-sourcing systems, studies [6, 49] show that drivers' trip acceptance depends on profitability, pickup distance, and surge pricing, which in turn affect wait times and throughput. In parking systems [26], drivers often ignore digital guidance due to outdated data or habitual preferences. In crowd-sourced delivery [21], couriers reject orders when incentives misalign with perceived effort. In energy and EV-charging coordination, scheduling frameworks remain strategy-proof only under truthful participation and fail to reassign resources once users deviate [5]. Collectively, these studies highlight that effective CPS coordination must adapt to, rather than enforce, user behavior, motivating fast post-deviation reassignment.

2.2 Dynamic Resource Allocation in CPS

Cooperative and optimization frameworks have significantly advanced resource allocation in UAV-enabled CPS. Game-theoretic models achieve Pareto-efficient sharing of communication and control resources via Nash bargaining and cooperative task assignment [56], while multi-UAV systems employ energy-aware clustering and Shapley value-based fairness for balanced exploration and workload [18]. Complementary optimization schemes integrate goal-oriented bandwidth control and hybrid FDMA-NOMA trajectory planning to jointly minimize energy consumption and latency in aerial sensing networks [39].

Recent studies extend CPS coordination to energy infrastructures, emphasizing adaptive control, distributed optimization, and resilience. Reinforcement learning-based digital twin frameworks improve grid efficiency under dynamic conditions [52], while the integrated edge-fog architectures enable secure, low-latency, and energy-aware decisions with renewable-powered AI sensing [23]. Inverter-based microgrids use event-triggered distributed control for voltage-frequency stability under communication delays [51].

EV charging systems exemplify the challenges of large-scale CPS coordination, where real-time scheduling must balance user preferences and infrastructure constraints. Multi-objective models optimize charger selection by distance, state-of-charge (SoC), and capacity [4], while distributed coordination schemes balance grid load through localized decisions [37]. Transactional formulations integrate renewables, pricing, and user preferences via robust optimization [28]. Recent V2V charge-sharing frameworks model donor–acceptor pairing as a stable matching problem under communication limits, enabling decentralized energy exchange [10].

2.3 Exchange and Matching Mechanisms in CPS

Matching theory provides foundational tools for stable and fair resource assignment in multi-agent systems. The Deferred Acceptance algorithm [17] and Top-Trading-Cycles (TTC) mechanism [41] ensure stability and strategy-proofness under single ownership. While several TTC extensions expand their theoretical scope, none address post-deviation reassignment in capacity-constrained CPS settings. For instance, [3] generalized TTC to account for preference heterogeneity, [40] incorporated priority fairness through the concept of justness, and [19] introduced an equitable variant that eliminates avoidable envy. More recent efforts adapt TTC to social and networked environments, restricting trades to neighboring agents [30, 53]. However, these frameworks assume static ownership and perfect compliance, limiting adaptability after reassignment. The closest work to ours is [8] that studies markets in which each agent may have multiple endowments, whereas we only consider a single one. In contrast to these existing strategies, our capacity-aware TTC framework retains key theoretical guarantees while enabling decentralized, preference-driven reassignment in dynamic, shared-resource CPS environments.

2.4 Research Gaps

Existing studies reveal four key gaps: (1) CPS coordination assumes full compliance with no post-deviation reassignment [15, 31]; (2) TTC models address only one-to-one ownership, ignoring capacity-constrained settings [41]; (3) one-to-many mechanisms like DAA ensure stability but not Pareto optimality [17]; and (4) most CPS schedulers rely on centralized recomputation [39, 56]. We address these through a capacity-aware, TTC framework preserving theoretical guarantees under non-compliance.

3 System Model and Problem Formulation

3.1 System Model

We consider a CPS platform coordinating a set of agents $\mathcal{A} = \{a_1, a_2, \dots, a_{|\mathcal{A}|}\}$ denoting the set of autonomous or human-in-the-loop *agents* (e.g., vehicles, UAVs, responders, or service units) that access a set of shared *resources* $\mathcal{R} = \{r_1, r_2, \dots, r_{|\mathcal{R}|}\}$ (e.g., charging ports or service nodes). Each resource $r_j \in \mathcal{R}$ possesses a finite capacity $q_j \in \mathbb{Z}^+$, indicating the number of agents that can be simultaneously served or accommodated. Collectively, these form the quota vector $\mathbf{q} = (q_1, q_2, \dots, q_{|\mathcal{R}|})$. During the assignment process, the quota vector \mathbf{q} is updated by decrementing q_j whenever an agent is allocated to r_j .

At any decision epoch, an assignment procedure is assumed to be in place to produce an initial one-to-many allocation $\omega : \mathcal{A} \rightarrow \mathcal{R} \cup \{\emptyset\}$, where $\omega(a_i) = r_j$ denotes that agent a_i is assigned to resource r_j , and $\omega(a_i) = \emptyset$ represents unassigned agents

or idle capacity. Agents may either *comply* with their assigned resource or *deviate* based on their real-time preferences, local context, or behavioral state. We capture such non-compliant agents in $\mathcal{A}^{\text{nc}} = \{a_i \in \mathcal{A} : a_i \text{ rejects } \omega(a_i)\}$, and subsequently, the compliant agents are captured in $\mathcal{A}^c = \mathcal{A} \setminus \mathcal{A}^{\text{nc}}$. Thus, the reassignment mechanism operates exclusively over non-compliant agents \mathcal{A}^{nc} and the residual capacity vector \mathbf{q} , while ensuring that allocations of compliant agents remain untouched.

After identifying the non-compliant agents \mathcal{A}^{nc} , each agent $a_i \in \mathcal{A}^{\text{nc}}$ is allowed to seek an alternative allocation based on its current operational context. However, not all resources may be admissible for every agent. We therefore define, for each such agent, a *feasible resource set* $\mathcal{R}_i^{\text{feas}} \subseteq \mathcal{R}$, which captures the resources that a_i can legitimately access under the system's physical, temporal, or capacity constraints. A resource r_j is included in the feasible set $\mathcal{R}_i^{\text{feas}}$ for an agent a_i only if: (i) $q_j > 0$, ensuring at least one available unit of service; (ii) a_i can physically or temporally reach r_j within its operational limits (e.g., mobility, energy, latency); and (iii) r_j satisfies any agent-specific requirements such as charger type, task compatibility, or priority class. Note that these conditions naturally vary across CPS domains (e.g., an EV requiring a fast charger, a UAV constrained by remaining battery, or a responder restricted by response-time bounds). Our goal is not to enumerate domain-specific rules, but to ensure that only admissible options after excluding capacity consumed by compliant agents enter $\mathcal{R}_i^{\text{feas}}$.

Each non-compliant agent $a_i \in \mathcal{A}^{\text{nc}}$ reports a strict preference ordering over its feasible set $\mathcal{R}_i^{\text{feas}} \subseteq \mathcal{R}$. This ordering is captured as $r_1 \succ_i r_2 \succ_i \dots \succ_i r_{|\mathcal{R}_i^{\text{feas}}|}$, where r_1 and $r_{|\mathcal{R}_i^{\text{feas}}|}$ is the most and least preferred respectively. Together we use $P(a_i)$ to capture this ordinal relationship of a_i . Preferences can be generated using domain-specific factors (e.g., detour, latency, energy, task fit), but the mechanism uses only the ordering over $\mathcal{R}_i^{\text{feas}}$.

3.2 Mapping Ranks to Satisfaction

Given a preference ordering $P(a_i)$ over the feasible set $\mathcal{R}_i^{\text{feas}}$, each resource in this ordering is mapped to a numerical rank through a function $\text{rank}_i : \mathcal{R}_i^{\text{feas}} \rightarrow \{1, 2, \dots, |\mathcal{R}_i^{\text{feas}}|\}$, where $\text{rank}_i(r_j) = 1$ denotes the most preferred resource according to $P(a_i)$. This ranking actually reflects the level of satisfaction of an agent with the final assignment and can be computed in different ways. Some works [9, 47, 48] compute the satisfaction score is the normalized linear form as shown in Eq. (1), where $s_i(r_j) = 1$ is for the top-ranked choice and $s_i(r_j) = 0$ for the least preferred.

$$s_i(r_j) = \frac{|\mathcal{R}_i^{\text{feas}}| - \text{rank}_i(r_j)}{|\mathcal{R}_i^{\text{feas}}| - 1} \quad (1)$$

Let us consider an agent a_1 with preference ordering $P(a_1) : r_1 \succ r_2 \succ r_3 \succ r_4$. Adopting Eq. (1), the satisfaction values become for different assignments are $s_1(r_1) = 1.00$, $s_1(r_2) = 0.67$, $s_1(r_3) = 0.33$, and $s_1(r_4) = 0.00$. Thus, assigning a_1 to its first, second, third, or fourth choice yields 100%, 67%, 33%, and 0% satisfaction respectively. Although the linear score provides a simple normalization of ranks, it fails to capture key aspects of human decision behavior. *First*, it assumes uniform sensitivity across ranks, whereas empirical studies [35, 36, 55] show that diminishing sensitivity exists, with improvements near the top matter disproportionately more than improvements near the bottom. *Second*, it is reference-blind: an

agent's satisfaction depends only on the assigned rank, not on how that outcome compares to its initial allocation or expectation. *Third*, it cannot model threshold effects (e.g., sharp drops beyond a top- k acceptable set), nor can it ensure comparability across agents with differently sized feasible sets. These limitations motivate a richer, reference-dependent formulation based on Prospect Theory (PT) [35] that incorporates diminishing sensitivity and gain-loss asymmetry while preserving ordinal preference structure.

3.3 Prospect-Theoretic Satisfaction Model

PT models human evaluation of outcomes relative to a reference point rather than in absolute terms. The generic value function [29] is defined as Eq. (2), where z denotes the gain or loss relative to a reference point, α and β capture diminishing sensitivity for gains and losses, and λ models loss aversion.

$$v(z) = \begin{cases} z^\alpha, & z \geq 0, \\ -\lambda(-z)^\beta, & z < 0, \end{cases} \quad 0 < \alpha, \beta \leq 1, \lambda > 1, \quad (2)$$

In our CPS setting, each agent compares any reassigned resource to its initial endowment, which is considered the reference point. Let the linear satisfaction from assigning resource r_j to agent a_i be $s_i(r_j)$ (obtained from Eq. (1)), and define the reference satisfaction as $s_i^{\text{ref}} = s_i(\omega(a_i))$. The raw gain from receiving r_j is therefore $z_i(r_j) = s_i(r_j) - s_i^{\text{ref}}$. The overall goal of the re-assignment procedure is to never receive an assignment worse than their endowment; hence $z_i(r_j) \geq 0$ and the loss region of (2) is never invoked. Thus, only the gain-side curvature is relevant, yielding the trimmed form $v(z_i(r_j)) = (z_i(r_j))^\alpha$.

Additionally, it is worth noting that the agents may have different reference points s_i^{ref} , implying that the maximum achievable improvement also varies. To ensure comparability across heterogeneous agents, we normalize by the maximum possible gain: $z_i^{\text{max}} = 1 - s_i^{\text{ref}}$, $\hat{z}_i(r_j) = \frac{z_i(r_j)}{z_i^{\text{max}}} \in [0, 1]$. Thus, the final PT satisfaction obtained by a_i is derived as:

$$\text{Sat}_i(r_j) = (\hat{z}_i(r_j))^\alpha, \quad 0 < \alpha \leq 1. \quad (3)$$

This formulation preserves ordinal preferences while incorporating behavioral realism through (i) reference dependence, (ii) diminishing sensitivity, and (iii) fair normalization across agents with different feasible sets and endowment quality.

3.4 Problem Formulation

The reassignment procedure aims to boost/maximize the aggregate satisfaction of the non-compliant agents while ensuring feasibility and respecting all capacity constraints. For each non-compliant agent $a_i \in \mathcal{A}^{\text{nc}}$ and resource $r_j \in \mathcal{R}$, let $y_{i,j} \in \{0, 1\}$ be a binary indicator variable capturing the reassignment of a_i to r_j . The objective as expressed in Eq. (4) is to maximize the aggregate PT satisfaction. Constraint (5) ensures that each non-compliant agent is assigned to at most one resource. On the other hand, Constraint (6) enforces that no resource exceeds its capacity. Constraint (7) restricts assignments to only those resources that are feasible for each agent. Constraint (8) guarantees that the non-compliant agents are never worse-off by preventing assignments that yield lower satisfaction than the agent's initial endowment. Constraint (9) specifies that all assignment decisions are binary.

$$\text{maximize} \quad \sum_{a_i \in \mathcal{A}^{\text{nc}}} \sum_{r_j \in \mathcal{R}} \text{Sat}_i(r_j) \times y_{i,j} \quad (4)$$

$$\text{s.t.} \quad \sum_{r_j \in \mathcal{R}} y_{i,j} \leq 1, \quad \forall a_i \in \mathcal{A}^{\text{nc}} \quad (5)$$

$$\sum_{a_i \in \mathcal{A}^{\text{nc}}} y_{i,j} \leq q_j, \quad \forall r_j \in \mathcal{R} \quad (6)$$

$$y_{i,j} = 0, \quad \forall a_i \in \mathcal{A}^{\text{nc}}, \forall r_j \notin \mathcal{R}_i^{\text{feas}} \subseteq \mathcal{R} \quad (7)$$

$$\text{Sat}_i(r_j) \times y_{i,j} \geq \text{Sat}_i(\omega(a_i)), \quad \forall a_i \in \mathcal{A}^{\text{nc}} \quad (8)$$

$$y_{i,j} \in \{0, 1\}, \quad \forall a_i \in \mathcal{A}^{\text{nc}}, \forall r_j \in \mathcal{R} \quad (9)$$

Instead of relying on centralized optimization, the next section demonstrates how a capacity-aware extension of the TTC mechanism produces these assignments in a preference-consistent manner while respecting the constraints.

4 Proposed Solution

4.1 Resource Allocation as Assignment Problem

DEFINITION 1 (PREFERENCES). *Each non-compliant agent $a_i \in \mathcal{A}^{\text{nc}}$ reports a strict preference ordering \succ_{a_i} over its feasible option set denoted by $\mathcal{R}_i^{\text{feas}} \subseteq \mathcal{R}$.*

DEFINITION 2 (ASSIGNMENT). *An assignment is a one-to-many mapping $\mu : \mathcal{A}^{\text{nc}} \cup \mathcal{R} \rightarrow 2^{\mathcal{A}^{\text{nc}}} \cup 2^{\mathcal{R}}$ satisfying: (i) $\forall a_i \in \mathcal{A}^{\text{nc}}, |\mu(a_i)| \leq 1$ and $\mu(a_i) \subseteq \mathcal{R}$, (ii) $\forall r_j \in \mathcal{R}, |\mu(r_j)| \leq q_j$ and $\mu(r_j) \subseteq \mathcal{A}^{\text{nc}}$, (iii) $a_i \in \mu(r_j) \iff r_j \in \mu(a_i)$.*

DEFINITION 3 (PARETO OPTIMALITY). *An assignment μ is Pareto optimal if there exists no feasible assignment μ' such that: $\exists a_i$ with $\mu'(a_i) \succ_{a_i} \mu(a_i)$; and $\forall a_{i'} \neq a_i, \mu'(a_{i'}) \succeq_{a_{i'}} \mu(a_{i'})$. Thus, μ' makes at least one agent strictly better off without making others worse off.*

DEFINITION 4 (INDIVIDUAL RATIONALITY). *With ω capturing the initial endowment mapping $\omega : \mathcal{A}^{\text{nc}} \rightarrow \mathcal{R} \cup \{\emptyset\}$. An assignment μ is individually rational if $\mu(a_i) \succeq_{a_i} \omega(a_i), \forall a_i \in \mathcal{A}^{\text{nc}}$. Thus, no agent is worse off than its initial endowment.*

DEFINITION 5 (CORE STABILITY). *Let $\mathcal{A}' \subseteq \mathcal{A}^{\text{nc}}$ and $\mathcal{R}' = \{\omega(a_i) \mid a_i \in \mathcal{A}'\}$ be their endowed resources. An assignment μ is core stable if there is no coalition $(\mathcal{A}', \mathcal{R}')$ and feasible reassignment μ' such that $\mu'(a_i) \succ_{a_i} \mu(a_i), \forall a_i \in \mathcal{A}'$. That is, no subset of agents can mutually reassign only their endowed resources and all become strictly better off.*

DEFINITION 6 (STRATEGY-PROOFNESS). *A mechanism is strategy-proof if no agent can obtain a strictly better assignment by mis-reporting. Let μ be the allocation under the true preference profile $(\succ_{a_i})_{a_i \in \mathcal{A}^{\text{nc}}}$, and μ' be the allocation when some agent a_i misreports \succ'_{a_i} , while others report truthfully. The mechanism is strategy-proof if, for every agent a_i , $\mu(a_i) \succeq_{a_i} \mu'(a_i)$, where \succeq_{a_i} is a_i 's true preference.*

4.2 TTC: Limitations in Constrained CPS

To illustrate the working of TTC, consider a simple one-to-one exchange market with three agents $\mathcal{A} = \{a_1, a_2, a_3\}$ and three resources $\mathcal{R} = \{r_1, r_2, r_3\}$, where each has unit capacity ($q_j = 1$). Each agent's endowments and preferences is shown in Table 2a. Using

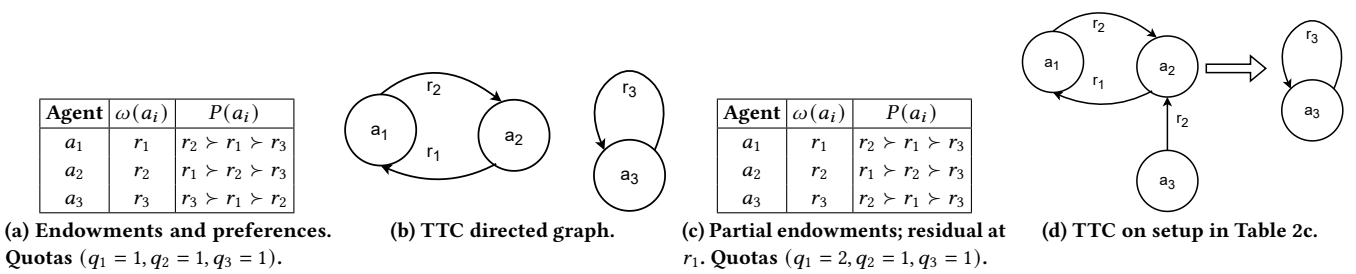
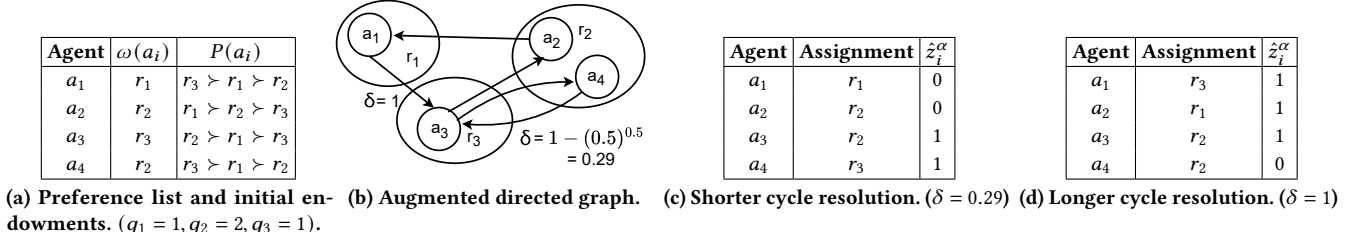
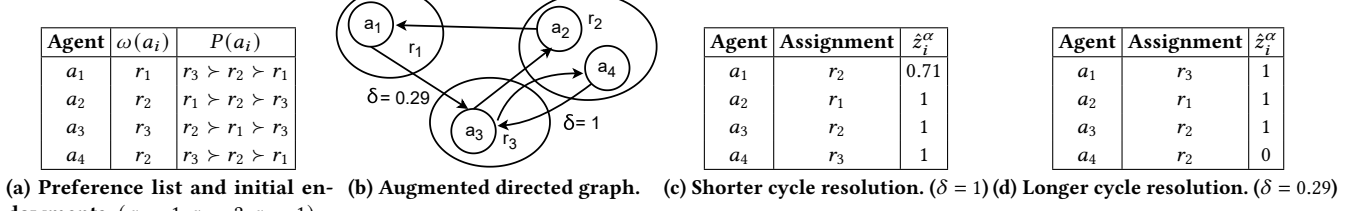


Figure 2: TTC example instances with full and partial endowments.

Figure 3: Case A, example 1: Preferences, augmented graph, and the final satisfactions ($\alpha = 0.5$).Figure 4: Case A, example 2: Preferences, augmented graph, and the final satisfactions ($\alpha = 0.5$).

the instance in Table 2a, the TTC procedure begins constructing a graph, where the agents (a_i) are represented by vertices in a graph. In the first step (graph construction), each agent points to the owner of its most preferred resource via a directed edge. For example, a_1 points to a_2 , the owner of its most preferred resource r_2 . This step leads to addition of the directed edges $(a_1 \rightarrow a_2)$, $(a_2 \rightarrow a_1)$, and $(a_3 \rightarrow a_3)$ (self-loop) as shown in Fig. 2b. At the end of graph construction, the graph must contain at least one cycle [41]. For instance, Fig. 2b has two cycles $(a_1 \rightarrow a_2 \rightarrow a_1)$ and $(a_3 \rightarrow a_3)$. In the next step (cycle resolution), the trade is conducted among the agents in a cycle by reassigning resources to the individuals who pointed to the current owner. For instance, by resolving the first cycle, a_1 receives r_2 and a_2 receives r_1 ; both agents and resources are then removed from further consideration. Similarly, the other cycle is also resolved. Therefore the final allocation is $\mu(a_1) = r_2$, $\mu(a_2) = r_1$, and $\mu(a_3) = r_3$. The outcome of TTC in the above example satisfies all the properties established previously [34].

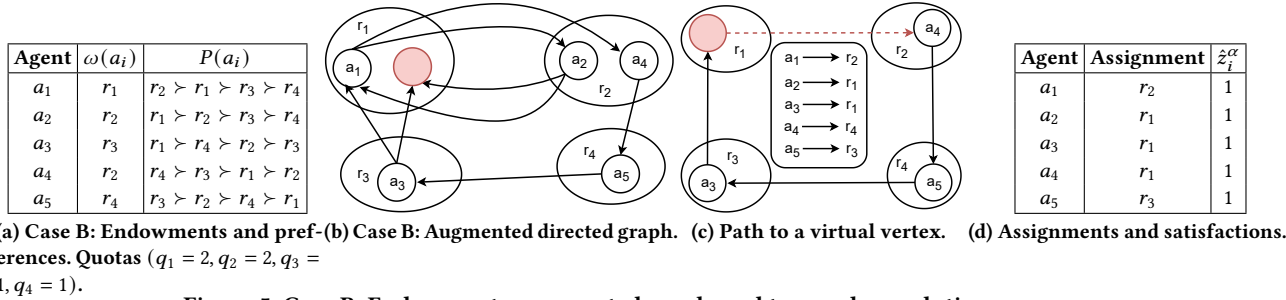
On the other hand, let Table 2c represent another setup, where the capacity of resource r_1 is 2, and the preference of a_3 is $r_2 \succ r_1 \succ r_3$. In this changed setup, the classical TTC leads to the final assignment $\mu(a_1) = r_2$, $\mu(a_2) = r_1$, and $\mu(a_3) = r_3$ as depicted in Fig. 2d. Since TTC operates only on endowed units, the spare slot at r_1 remains “invisible”, causing a_3 to be assigned to r_3 even though it strictly prefers r_1 , where a slot is still available. This assignment is *core-stable* in the endowment sense, since the spare capacity at r_1 has no owner and thus cannot participate in any blocking coalition. However, in capacity-constrained CPS, this notion of *core-stability*

is inefficient and misaligned, as the unowned capacity represents real, usable supply. Such an assignment can be improved by a direct assignment of a_3 to r_1 , without harming any other agent, and thus the current assignment violates the *Pareto optimality*. Although a direct reassignment resolves the issue in this simple example, the situation becomes more complex when multiple agents compete for the same available resource, necessitating novel approaches to assignment.

4.3 Solution Approach

Case A (Co-ownership): We begin by modifying the standard TTC graph construction [41]. Each resource is treated as a meta-node containing its initially endowed agents as interior nodes. For example, in Fig. 3, resource r_2 becomes a meta-node whose components are agents a_2 and a_4 , as listed in Table 3a. The same procedure applies to all resources. Next, each agent draws directed edges toward the owners of its top preference. This is the key departure from classical TTC, which restricts agents to a single outgoing edge under atomic (one-to-one) ownership. In our setting, resources may be co-owned. For instance, r_2 is jointly owned by a_2 and a_4 (Fig. 3). Therefore, if an agent’s preferred resource is co-owned, as in the case of a_3 , we draw one edge to each owner (a_2 and a_4). For single-owner resources, we draw one edge following the classical TTC rule. The resulting directed graph is shown in Fig. 3b.

We now turn to cycle resolution, which becomes substantially more intricate in our setting. In contrast to classical TTC, where each agent has exactly one outgoing edge and all cycles are therefore



(a) Case B: Endowments and preferences. Quotas ($q_1 = 2, q_2 = 2, q_3 = 1, q_4 = 1$).

Figure 5: Case B: Endowments, augmented graph, and two cycle-resolution sequences.

vertex-disjoint, we allow multiple outgoing edges, which enables the formation of overlapping cycles. As illustrated in Fig. 3b, two cycles coexist: a shorter cycle ($a_3 \rightarrow a_4 \rightarrow a_3$) and a longer cycle ($a_1 \rightarrow a_3 \rightarrow a_2 \rightarrow a_1$), with agent a_3 appearing in both. This overlap makes the resolution order decisive. Resolving the shorter cycle first leads to an assignment (Table 3c) with a cumulative satisfaction score of 2. Whereas prioritizing the longer cycle produces the assignment shown in Table 3d, and it leads to a higher cumulative satisfaction than the previous assignment. However, if the preference lists are changed slightly as Table 4a, the same cycle resolution for the augmented graph (Fig. 4b) provides an opposite result. From the assignment Tables 4c and 4d, it is evident that in this example, resolving the shorter cycle first leads to a better total satisfaction. These observations underscore that, unlike classical TTC, the cycle-resolution order has a critical impact on overall satisfaction, and finding the optimal ordering is non-trivial. Overlapping cycles, competing improvements, and interdependencies across edges create a combinatorial search space, which is challenging to solve.

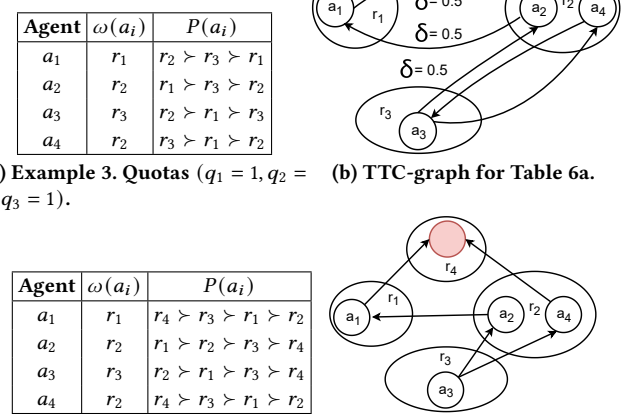
Instead of finding a global cycle resolution order through exhaustive search, we develop a heuristic that optimizes satisfaction locally in each round of TTC. We notice that resolving a cycle c_1 among multiple cycles $\{c_1, \dots, c_n\}$ overlapping at vertex a_i impacts the satisfaction of its immediate predecessor vertices $a_k \in \{c_2, \dots, c_n\}$ as resolving c_1 removes the edge $(a_k \rightarrow a_i)$ and forces a_k to move to its next choice in the preference list. We capture this impact on the satisfaction of immediate predecessors through the *minimum satisfaction loss* δ , defined as the difference between the satisfaction of obtaining the currently chosen resource and that of obtaining the next preferred resource. Therefore, prioritizing the resolution of cycles with larger δ minimizes the satisfaction loss of the predecessors and locally maximizes the satisfaction. In Fig. 3 and 4, resolving the cycles according to δ yields higher cumulative satisfaction.

Case B (No ownership/ Partial ownership): This case considers a scenario where the resources are not at capacity, and there is at least a vacant slot which is preferred by some agent. As the classical TTC cannot handle empty slots, we consider a virtual agent owner per empty slot (indicated by a red circle in Fig. 5b) to force the involvement of empty slots in the trading. Consequently, by following the graph construction step of TTC from Table 5a, we get a directed graph (Fig. 5b) with two cycles, $(a_1 \rightarrow a_2 \rightarrow a_1)$ and $(a_1 \rightarrow a_4 \rightarrow a_5 \rightarrow a_3 \rightarrow a_1)$.

However, since virtual owners have no preferences, they have no outgoing edges and therefore cannot be part of any cycle. Hence, regardless of the order of resolution, resolving all cycles results in a directed acyclic graph (DAG) whose paths terminate at virtual agent

vertices. In our example, resolving the cycle $(a_1 \rightarrow a_2 \rightarrow a_1)$ yields the path $a_4 \rightarrow a_5 \rightarrow a_3 \rightarrow a^v$ (Fig. 5c). The assignment trades along any path ending at a virtual vertex can then be implemented in one step by creating a cycle, that is, by adding an edge from the virtual vertex a^v to the starting vertex of the path a_4 in the example.

If there exist multiple paths to a virtual vertex, they overlap at least at the virtual vertex, and their resolution order can be determined by computing the *minimum satisfaction loss* δ of the immediate predecessors of the overlapping vertex, similar to case A. For both Cases A and B, if there exist multiple overlapping vertices (Fig. 6), the ordering can be determined by taking the sum of the minimum satisfaction losses.



(a) Example 3. Quotas ($q_1 = 1, q_2 = 2, q_3 = 1$). (b) TTC-graph for Table 6a.

(c) Example 4. Quotas ($q_1 = 1, q_2 = 2, q_3 = 1, q_4 = 1$). (d) TTC-graph for Table 6c.

Figure 6: TTC-graph for multiple overlapping vertices.
ReACT-TTC: To efficiently handle Cases A, B, and their combinations, here we formally design ReACT-TTC (Algorithm 1). It consists of three major steps that repeat until all agents have obtained their final resource assignment.

Step 1 (Graph Construction). At each iteration, this step considers all the agents without a final assignment as a vertex set V . Next, it constructs directed edges from each agent a_i to the owner of its most preferred resource if the agent does not have any existing outgoing edge (i.e., the outgoing neighbor set $N^-(a_i) = \emptyset$). If a resource with empty slots is preferred at this iteration, virtual owner vertices are added (Algorithm 1 Line 7-11). For each edge $(a_i \rightarrow a_k)$, the edge weight is assigned to the minimum satisfaction loss computed as $\delta(a_i, r_j) = \hat{z}_i^\alpha(r_j) - \hat{z}_i^\alpha(r_j^{next})$, where r_j, r_j^{next} are the current and next resource preference of a_i , and $\hat{z}_i^\alpha(r_j), \hat{z}_i^\alpha(r_j^{next})$ are their

related satisfactions, respectively. The graph $G(V, E)$ is used in the algorithm, where E denotes the set of edges.

Step 2 (Complete Cycle Resolution). This step finds the simple cycles [27] in the directed graph G and sorts them in decreasing order of their total satisfaction loss computed as $\sum_{a_i \in O} \delta(a_i, r_j)$, where O is the set of overlapping vertices in a cycle c . Then the cycles are resolved using Algorithm 2 by following the sorted order. For each edge $(a_i \rightarrow a_i')$ in a cycle, the resolution stage assigns the current resource of a_i' to a_i as the final assignment $\mu(a_i)$ and updates the current assignment of the resource (Algorithm 2 Line 4–10). If a resource obtains final assignments for all its slots, it is removed from the preference lists of all agents. Finally, after resolving a cycle c , all of its vertices are removed from the graph.

Step 3 (Incomplete Cycle Resolution). Completing all cycles in Step 2 makes G a DAG. Step 3 finds all the directed paths ending at the virtual vertices and sorts them in decreasing order of their total satisfaction loss. Next, each path from the sorted list of paths is processed, and the end vertex (virtual) is connected with the starting vertex of the path. It leads to a cycle, which is resolved using Algorithm 2 to obtain the final assignments of the agents along the path. As in Step 2, at the end, all vertices on the path are removed from the graph.

These steps continue until all agents receive their final assignments or their preference lists are exhausted.

Time Complexity Analysis. Algorithm 1 Step 1 takes $O(q_{max} \cdot |\mathcal{A}^{nc}|)$ time, where q_{max} is the maximum capacity of any resource and \mathcal{A}^{nc} is the total agents in the system. Step 1 creates a graph of $O(|\mathcal{A}^{nc}|)$ vertices and $O(q_{max} \cdot |\mathcal{A}^{nc}|)$ edges. Therefore, finding all the cycles in a round of ReACT-TTC can take $O(|V| + |E|)(|C|) = O(q_{max} \cdot |\mathcal{A}^{nc}|^2)$ time. Finding the satisfaction loss and sorting the cycles takes $O(|\mathcal{A}^{nc}| \cdot \log(|\mathcal{A}^{nc}|))$ time. Resolving a cycle takes $O(|\mathcal{A}^{nc}|)$ time. Step 3 requires the same time complexity as Step 2. If the termination of ReACT-TTC requires $|\mathcal{A}^{nc}|$ rounds, the worst case complexity of the algorithm will be $O(|\mathcal{A}^{nc}| \cdot (q_{max} \cdot |\mathcal{A}^{nc}|^2 + |\mathcal{A}^{nc}| \cdot \log(|\mathcal{A}^{nc}|)) = O(q_{max} \cdot |\mathcal{A}^{nc}|^3)$.

5 Theoretical Analysis

THEOREM 1 (TERMINATION). *TTC terminates after a finite number of rounds and returns a feasible assignment.*

PROOF. For a round t in TTC, let $\mathcal{A}' \subseteq \mathcal{A}^{nc}$ be the set of unassigned agents. Each agent $a_i \in \mathcal{A}'$ points to the owner of its top remaining acceptable resource (denote this resource by r'), which is either (i) owned by one or more agents in \mathcal{A}' , or (ii) unowned. Accordingly, we construct a directed graph on vertex set $\mathcal{A}' \cup \{\phi\}$, where ϕ represents all unowned resources:

- (i) If r' is owned by an agent a_j , we add a directed edge $a_i \rightarrow a_j$.
- (ii) If r' is co-owned by $|q_{r'}|$ agents, we add $|q_{r'}|$ such edges.
- (iii) If r' is unowned, we add a single edge $a_i \rightarrow \phi$.

In case (i), every agent in \mathcal{A}' has out-degree at least one, so the resulting finite digraph contains a directed cycle [7]. Each such cycle (including overlapping cycles resolved as in Case A of Section 4.3) is executed via a TTC rotation, which assigns resources to the agents on the cycle and removes them from the market.

In case (ii), ϕ has out-degree zero, and any directed walk ending at ϕ defines an agent ϕ chain beginning at an agent with no incoming edges. We close the chain into a directed cycle by adding an auxiliary

Algorithm 1: ReACT-TTC

```

Input:  $\mathcal{A}^{nc}, \mathcal{R}$ 
Output:  $\mu : \mathcal{A}^{nc} \cup \mathcal{R} \rightarrow 2^{\mathcal{A}^{nc} \cup \mathcal{R}}$ 
1 Initialize a graph  $G(V, E)$  such that  $V = \mathcal{A}^{nc}$  and  $E = \emptyset$ 
2 Initialize a set of virtual vertices  $V' = \emptyset$ 
3 while True do
    /* Step 1: Graph Construction */
    4 for  $a_i \in V \setminus V'$  do
        5   if  $N^-(a_i) = \emptyset$  and  $P(a_i) \neq \emptyset$  then
            6     Preferred resource  $r_j \leftarrow \text{Extract}(P(a_i))$ 
            7     /* Create Virtual Vertices */
            8     Available quota  $\epsilon \leftarrow q_j - |\omega(r_j)|$ 
            9     if  $\epsilon > 0$  then
                10       Create virtual vertices  $\{a_1^r, \dots, a_\epsilon^r\}$ 
                11       Add virtual vertices to  $V, V'$ , and  $\omega(r_j)$ 
                12        $\omega(a_k^r) \leftarrow r_j \ \forall a_k^r \in \{a_1^r, \dots, a_\epsilon^r\}$ 
                13     /* Add Directed Weighted Edges */
                14     for  $a_k \in \omega(r_j)$  do
                    15       Add directed edge  $(a_i \rightarrow a_k)$  with edge weight
                    16        $\delta(a_i, r_j)$  to  $E$ 
    /* Step 2: Complete Cycle Resolution */
    17    $C \leftarrow \text{Find\_simple\_cycles}(G(V, E))$ 
    18   Sort the cycles in  $C$  in decreasing order of their total
        satisfaction loss
    19   for cycle  $c$  in sorted  $C$  do
        20     if any vertex in  $c$  does not exist in  $V$  then
        21       Skip
        22       Resolve_cycle( $c, \mu, \omega$ )
        23       Remove all vertices in  $c$  from  $G(V, E)$ 
    /* Step 3: Incomplete Cycle Resolution */
    24    $\mathcal{L} \leftarrow \text{Find directed paths ending at virtual vertices } V'$  in
        directed acyclic graph  $G(V, E)$ 
    25   Sort the paths in  $\mathcal{L}$  in decreasing order of their total
        satisfaction loss
    26   for paths  $t$  in sorted  $\mathcal{L}$  do
        27     if any vertex in  $t$  does not exist in  $V$  then
        28       Skip
        29        $c \leftarrow \text{Create a cycle by adding a directed edge from the last}$ 
        30        $\text{vertex to the first vertex of path } t$ 
        31       Resolve_cycle( $c, \mu, \omega$ )
        32       Remove all vertices in  $c$  from  $G(V, E)$ 
    /* Terminate Iterations */
    33   if  $|V \setminus V'| = 0$  or  $P(a_i) = \emptyset \ \forall a_i \in \mathcal{A}^{nc}$  then
        34     break to outer loop

```

edge $\phi \rightarrow a_{i_1}$, where a_{i_1} is the first agent on the chain, and apply a TTC rotation to reallocate one unowned resource (Case B of Section 4.3). This again removes at least one agent and its allocated resources from the market.

Both cases may occur simultaneously, but in every round, at least one agent is removed from \mathcal{A}' . Finiteness of \mathcal{A}' therefore implies that the procedure terminates after finitely many rounds, producing a feasible allocation. \square

Algorithm 2: Resolve_cycle(c, μ, ω)

```

1 for each edge  $(a_i \rightarrow a_{i'}) \in c$  do
2    $r_j \leftarrow \omega(a_j)$ 
3    $r_{j'} \leftarrow \omega(a_{i'})$ 
4   if  $a_i$  is not a virtual vertex then
5      $\mu(a_i) \leftarrow r_{j'}$ 
6      $\mu(r_{j'}) \leftarrow \mu(r_{j'}) \cup \{a_i\}$ 
7      $\omega(r_{j'}) \leftarrow \omega(r_{j'}) \setminus \{a_{i'}\}$ 
8     Update quota  $q_{j'} \leftarrow q_{j'} - 1$ 
9   else
10     $\omega(r_{j'}) \leftarrow \omega(r_{j'}) \setminus \{a_{i'}\} \cup \{a_i\}$ 
11   if  $q_{j'} = 0$  then
12     Remove  $r_{j'}$  from all preference lists  $P$ 

```

THEOREM 2 (INDIVIDUAL RATIONALITY). *The TTC outcome μ is individually rational: for every agent a_i , $\mu(a_i) \succeq_s \omega(a_i)$.*

PROOF. For a fixed round t and let \mathcal{A}' be the set of agents who are unassigned. Each $a_i \in \mathcal{A}'$ points to the owner of its top remaining acceptable resource r' , which is either (i) owned by one or more agents in \mathcal{A}' , or (ii) unowned (represented by a dummy vertex ϕ). This defines a directed graph on $\mathcal{A}' \cup \{\phi\}$.

(i) *An agent's endowed resource cannot be taken without the agent being part of the same resolved cycle.* Whenever a pointed resource is owned, an edge is drawn toward the owner of that resource. Thus, if an endowed resource $\omega(a_i)$ is allocated to another agent during a TTC rotation, that allocation must come from a directed cycle (Case A) or from a chain closed into a cycle (Case B). In either case, $\omega(a_i)$ is passed only to the predecessor of a_i on the cycle. Hence, if an agent's endowment leaves them, they must lie on that same cycle, ensuring no endowment is taken without including its owner. (ii) *When an agent exits, it receives its top remaining acceptable resource.* At the exit round, each agent a_i points to its top remaining acceptable resource r' , and by definition, the endowment $\omega(a_i)$ is still among its remaining acceptable resources until a_i exits. If r' is owned, the TTC rotation assigns a_i exactly r' , whether in a simple cycle, an overlapping cycle (Case A), or a cycle formed by closing a chain (Case B). If r' is unowned, the chain is closed into a cycle via $\phi \rightarrow a_i$, and the rotation again assigns a_i the unowned resource it pointed to. In the degenerate self-loop case, $r' = \omega(a_i)$, and a_i simply retains its endowment.

Thus, at its exit round, every agent receives exactly its top remaining acceptable resource, which is always weakly better than its endowment. Since each agent receives a resource that is weakly preferred to its endowment at the moment of exit, we have $\mu(a_i) \succeq_{a_i} \omega(a_i)$ for every agent a_i . Therefore, the final allocation is individually rational. \square

THEOREM 3 (PARETO OPTIMALITY). *The outcome of TTC, i.e., μ , is always Pareto optimal.*

PROOF. Let μ be the final allocation produced by the proposed algorithm, and suppose, for contradiction, that there exists a feasible allocation μ' that Pareto improves upon μ , i.e., $\mu'(a_{i'}) \succeq_{a_{i'}} \mu(a_{i'})$, $\forall a_{i'} \in \mathcal{A}^{\text{nc}} \setminus \{a_i\}$, and $\exists a_i$ such that $\mu'(a_i) \succ_{a_i} \mu(a_i)$. Among all agents who are strictly better off under μ' than μ , let a_i be the agent

who is removed *earliest* by our algorithm. Let r be a resource such that $r \in \mu'(a_i)$ and $r \notin \mu(a_i)$, and let $a_{i'}$ be the agent who receives r in the TTC round (say t_r). These allocations can be made via a simple cycle, an overlapping cycle, or a chain closing into a cycle.

Claim 1. *The resource r was still available at the round when a_i was removed by our algorithm.* If we assume the opposite, then r must have been allocated in an earlier round than t_r to some agent $a_{i'} \neq a_i$. Since μ' assigns r to a_i instead of $a_{i'}$, and μ' is a Pareto improvement over μ , agent $a_{i'}$ cannot be worse off under μ' . Because preferences are strict over individual resources, if $a_{i'}$ does not receive r in μ' , it must receive a resource that is strictly better than r . Thus, $a_{i'}$ is also strictly better off under μ' than under μ , and since r is allocated at round t_r , agent $a_{i'}$ must exit *no later* than a_i . This contradicts the choice of a_i as the strictly improving agent who exits earliest. Hence, r must have been available at the round when a_i was removed.

Claim 2. *At the round when a_i is removed, the algorithm assigns it a resource that is at least as preferred as r .* At its exit round, a_i points to its top remaining acceptable resource. Since r is available at this round by Claim 1, we have two possibilities: (a) a_i points directly to r . In this case, the cycle (or chain closed into a cycle) is executed in that round, assigning r to a_i immediately. (b) a_i points to some resource y with $y \succ_{a_i} r$. Then, in that round, the TTC rotation assigns y to a_i , and therefore a_i receives a resource strictly preferred to r . In all cases of the algorithm, i.e., simple cycles, overlapping cycles, and chain-cycles via the dummy vertex, the agent that was removed in that round receives exactly the resource it points to. Thus, at its exit, a_i receives a resource that is $\succeq_{a_i} r$.

Combining Claims 1 and 2, we conclude that at the round in which a_i is removed by our algorithm, a_i receives a resource that is $\succeq_{a_i} r$. But r is the resource that makes a_i strictly better off under μ' , so $\mu(a_i) \succeq_{a_i} r$ implies that $\mu(a_i) \succeq_{a_i} \mu'(a_i)$, contradicting the assumption that $\mu'(a_i) \succ_{a_i} \mu(a_i)$. Thus, no feasible allocation can strictly improve upon μ without making some agent worse off, and therefore μ is Pareto efficient. \square

THEOREM 4 (CORE STABILITY). *TTC outcome μ is in the core, implying no coalition $\mathcal{A}' \subseteq \mathcal{A}^{\text{nc}}$ can reassign its initially endowments so that every member of \mathcal{A}' is strictly better than under μ .*

PROOF. Assume, for contradiction, that there exists a non-empty coalition $\mathcal{A}' \subseteq \mathcal{A}^{\text{nc}}$ and a reassignment μ' that uses only the coalition's endowed units $W' = \{\omega(a_i) : a_i \in \mathcal{A}'\}$ and satisfies $\mu'(a_i) \succ_{a_i} \mu(a_i)$ for every $a_i \in \mathcal{A}'$. Let us consider an agent $a_i \in \mathcal{A}'$ who is removed *earliest* by the algorithm. Let $r = \mu'(a_i) \in W'$ be the resource that a_i would receive under the blocking deviation.

(1) *All coalition endowments are still available when a_i exits.* In our setting, an endowed unit can be transferred only when the owner participates in a TTC cycle. Since a_i is the first member of \mathcal{A}' to exit, no other agent has exited before it. Therefore, none of the units in W' has been removed yet, and in particular r is still available when a_i is processed.

(2) *At its exit round, a_i receives its top remaining acceptable unit.* In that round's a_i points to the owner of its top remaining choice. The algorithm, whether it executes a simple cycle, an overlapping cycle, or a chain closed into a cycle, assigns it to a_i . Since r is available, two cases arise: (i) a_i 's top choice is r , and is assigned, so $\mu(a_i) = r$, contradicting $\mu'(a_i) \succ_{a_i} \mu(a_i)$. (ii) a_i 's top choice is y with $y \succ_{a_i} r$.

Then $\mu(i) = y \succ_{a_i} r = \mu'(a_i)$, contradicting that μ' makes every coalition member strictly better off.

Both cases contradict the assumption that μ' strictly improves every agent in \mathcal{A}' . Therefore, no such blocking coalition exists, and μ is in the core. \square

THEOREM 5 (STRATEGY-PROOFNESS). *The proposed algorithm is individually strategy-proof under strict preferences. For any agent a_i , holding all other reports fixed, truthful reporting yields an allocation that is at least as good for a_i (in its true preference order) as the allocation obtained under any misreport.*

PROOF. Let us fix the preference of all agents other than a_i . Then we consider two execution mechanisms *Truthful* (T), where a_i reports its true preference \succ_{a_i} , and *Misreport* (M), where its reported preference differs. For contradiction, we assume that in M, agent a_i receives a resource that a_i strictly prefers to the one received in T. Let t_r be the earliest round at which the two executions differ in the set of assignments made. By definition of t_r , the sets of remaining agents and resources at the start of t_r are identical in T and M, and so is the ownership.

(1) *Every directed cycle in round t_r contains a_i .* Under TTC implementation, if there existed a cycle that does not contain a_i , then this cycle would appear identically in both T and M, and the mechanism would execute it in both runs. This would imply that T and M make the same assignments in round t_r , contradicting the definition of t_r as the first round where the assignments differ. Hence, every cycle present in round t_r must contain a_i .

(2) *In T, a_i receives its top remaining acceptable resource at round t_r .* Let r^* denote a_i 's top remaining acceptable choice at the start of t_r , according to its true preference order \succ_{a_i} . In the truthful execution T, agent a_i points to the owner of r^* . By (1), any cycle executed in round t_r must contain a_i , and TTC assigns to a_i exactly what it points to on that cycle. Therefore, in T, a_i receives r^* at round t_r .

(3) *a_i cannot strictly improve in M.* At round t_r , the set of remaining resources is the same in T and M, so any resource that a_i can receive in M at round t_r is among the same remaining units considered in T. By definition of r^* , we have $r^* \succ_{a_i} r$ or $r^* = r$ for every other remaining resources r . Thus, whatever unit a_i receives in M at round t_r is weakly worse than r^* in \succ_{a_i} . Since in T, a_i receives r^* , agent a_i cannot obtain a resource that is strictly preferred to its T-assignment by misreporting, contradicting the assumption.

Hence, no misreport by a_i can make a_i strictly better off, and the mechanism is individually strategy-proof. \square

6 Experimental Results

This section presents the experimental environment used to validate our approach in a realistic intelligent transportation system. We model an operational electric vehicle (EV)-charging CPS in which EVs interact with charging points (CPs) under heterogeneous preferences, varying compliance behavior due to dynamically evolving system states. The system is viewed as an assignment environment, where EVs constitute set of agents and CPs form the resources, with each CP with a quota $q_j \geq 1, \forall r_j \in \mathcal{R}$. Consistent with existing literature, several charge recommendation algorithms generate initial EV-CP assignments. However, these recommendations are typically system-centric and based on static assumptions, which may lead to non-compliance from human drivers. When an EV user chooses not

to comply with the initial recommendation, our proposed REACT-TTC mechanism incorporates the user's current preferences and computes an improved, preference-aligned reassignment without impacting the assignment of the compliant users.

6.1 Environmental Setup

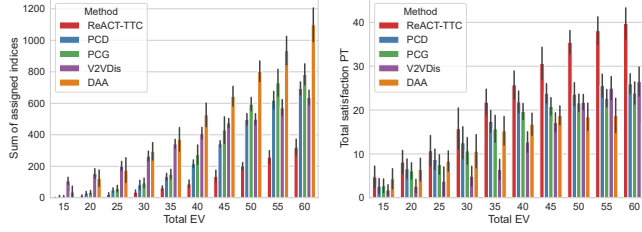
All simulations were implemented in Python 3.8.3, with EVs and CPs represented as independent object classes. The implementation of the REACT-TTC and the baselines is available at [24].

Dataset Description: To evaluate REACT-TTC under realistic operating conditions, we use a benchmark derived from the real-world JD Logistics distribution network in Beijing [57]. The dataset contains actual delivery and pickup requests, from which we sample locations to construct problem instances of varying sizes, each paired with a fixed set of charging stations. The dataset provides the geographic coordinates of all EV and CP nodes, along with pairwise travel distances and travel times that may violate the triangle inequality, reflecting real-world conditions of urban mobility. EV energy consumption parameters and charging characteristics are taken directly from the dataset's operational estimates. As a result, the generated scenarios capture realistic spatial structures, demand patterns, and travel behaviors, which are suitable for evaluating EV-CP assignment and reassignment mechanisms.

Baseline Algorithms: To evaluate the effectiveness of REACT-TTC, we compare it against three state-of-the-art matching-based approaches. V2VDisCS [10] formulates V2V charge sharing as a stable matching problem on bipartite graphs, solved via integer linear programming with low-overhead distributed heuristics in limited-communication settings. DAA [1] assigns EVs to roadside resources via a stable matching framework. For fairness, we use the same EV preference model and generate CP preferences by sorting EVs based on their maximum charging needs. SMEVCA [33] models EV-CP assignment as a one-to-many matching game under a subscription-driven SLA framework, using roadside units to form coalitions through two strategies: a fast greedy heuristic (PCG) and a more computation-intensive dynamic optimizer (PCD). For fair comparison, we adopt the preference generation procedure of SMEVCA and the initial endowment is generated using a local search-based algorithm with the same objectives as in SMEVCA.

6.2 Results and Analysis

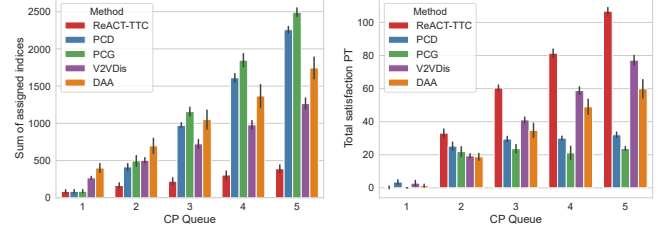
Fig. 7 illustrates the performance of different schemes with increasing non-compliant users. For this experiment, we assume the CP capacity $q_j = 2, \forall r_j \in \mathcal{R}$, hence the maximum limit (capacity constraint of the CPS system) is 60 EVs at full capacity. As shown in Fig. 7a, ReACT-TTC achieves the lowest aggregate rank sum, indicating consistently better allocations for non-compliant agents. This advantage stems from two key factors. *First*, TTC ensures Pareto-optimality by constructing directed graphs from each agent's most preferred choice, enabling mutually beneficial trades. *Second*, resolving overlapping cycles and chains prioritizes minimal satisfaction decay, consistently yielding lower-rank assignments. In contrast, baseline methods such as PCD, PCG, DAA, and V2VDisCS optimize system-centric metrics (e.g., detour distance, charging cost, or communication overhead) with limited regard for user satisfaction. Between these, PCG and PCD perform relatively better since their preference models align with system objectives, whereas



(a) Sum of Assigned Indices

(b) Satisfaction

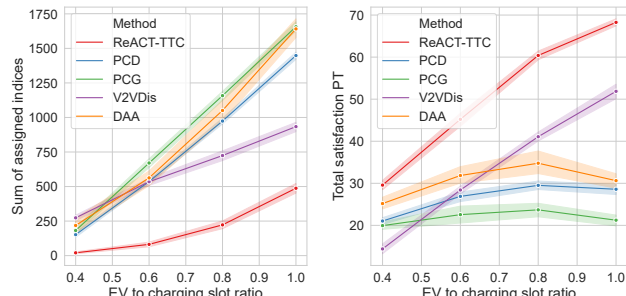
Figure 7: Analysis of satisfaction while varying the number of noncompliant EVs.



(a) Sum of Assigned Indices

(b) Satisfaction

Figure 8: Analysis of satisfaction while varying the size of the queue at a charging point. The non-compliant EV-to-total charging slot (Total CP * queue) ratio is fixed at 0.8.



(a) Sum of Assigned Indices

(b) Satisfaction

Figure 9: Analysis of satisfaction while varying the Non-compliant EV to total charging slot, i.e. $q_j = 3, \forall r_j \in \mathcal{R}$.

DAA and V2VDisCS lack such alignment, resulting in inferior satisfaction scores. Fig. 7b shows that ReACT-TTC consistently attains the highest PT-satisfaction, driven by factors discussed earlier.

Fig. 8 captures the aggregate ranks and the PT-satisfaction for different schemes for increasing queue size at the CPs, $q_j, \forall r_j \in \mathcal{R}$ for a constant ratio of non-compliance to total charging slot (= Total CP * queue), set to 0.8. In this case, referring to Fig. 8a, we observe an interesting behavior, where $q_j = 1, \forall r_j \in \mathcal{R}$. The sum of the satisfaction scores is at par with PCD and PCG, whereas the PT-satisfaction (Fig. 8b) observes an opposite behavior where PCD, PCG, and DAA attain better satisfaction. This is owing to the following two reasons. *Firstly*, ReACT-TTC takes Pareto optimal decisions to reduce the rank degradation, which may not necessarily align with the goal of maximizing the total satisfaction (Eq (4)) of the agents. *Secondly*, the gain in ReACT-TTC is computed with reference to the initial endowment, whereas for the others, any assignment beyond the reference point contributes to 0 satisfaction, reducing the negative impact beyond the endowments. Additionally, we observe that beyond $q_j \geq 2$, ReACT-TTC outperforms all baselines. As the queue size increases, the trade options for non-compliant agents also increase, thereby boosting the chances of better assignments. For the next set of experiments, we fix the queue size to $q_j = 3, \forall r_j \in \mathcal{R}$ and vary the ratio of non-compliance to the total number of charging slots. Across all schemes, the overall sum increases as the number of non-compliant users increases, as expected. It can also be observed from Fig. 9 that ReACT-TTC outperforms the baselines in both metrics (refer to Figs. 9a and 9b) considered earlier, for reasons explained earlier.

7 Discussions
ReACT-TTC provides an efficient reassignment mechanism, tested on EV-CP allocations under multi-quota constraints. While it maintains high satisfaction under non-compliance, some extensions can enhance its performance.

- **Cycle Sequencing Sensitivity:** The sequence of resolving overlapping cycles critically impacts system satisfaction. Dependencies and competing improvements across shared edges create a complex combinatorial space, making optimal ordering non-trivial. Developing principled sequencing strategies still remains an open challenge.
- **Parallel Cycle Detection:** Current cycle detection via depth-first search (DFS) is sequential and limits scalability in dense graphs. Parallelization could accelerate reassignment but may introduce conflicts across shared agents and edges. Safe coordination for parallel detection is a promising direction.
- **Learning-Based Preferences:** Although preferences are randomly generated for domain independence, real CPS systems provide data that can inform preference learning and better endowments. Incorporating such models can more accurately capture agent behavior and improve satisfaction.
- **Cross-Domain Evaluation:** Beyond the EV-CP setting, ReACT-TTC naturally extends to CPS domains where agents compete for limited resources and reassignment can improve system performance. In compute-task allocation, latency-sensitive tasks act as agents, and edge servers serve as resources; exchanging task-server assignments enables load consolidation and reduces queueing delay. In UAV bandwidth sharing, UAVs are agents, and communication channels are scarce resources; reallocating channel assignments can help mitigate interference hotspots and improve link stability. Such cross-domain evaluations can reveal domain-specific gains arising from reassignment.

8 Conclusions

This work presents a post-deviation reassignment framework tailored for shared-resource CPS in which user non-compliance is unavoidable. By extending the TTC mechanism to support many-to-one capacities and unassigned resources, we enable preference-driven reallocation that preserves core guarantees, including Pareto efficiency, individual rationality, and strategy-proofness. Our capacity-aware cycle-detection rules ensure correctness and termination, while integrating Prospect-Theoretic preferences provides a more

realistic model of user satisfaction. The framework operates independently of the initial allocation method, incurs minimal recomputations, and responds only when deviation occurs, making it suitable for real-time CPS environments. An evaluation of a real-world EV-charging scenario shows that the framework improves user satisfaction and assignment quality under heterogeneous behavior, highlighting its potential as a lightweight, domain-agnostic mechanism for resilient human-in-the-loop CPS.

References

- [1] Mahmuda Akter, Debjyoti Sengupta, Anurag Satpathy, and Sajal Das. 2024. Move: Matching game for partial offloading in vehicular edge computing. In *ICC 2024-IEEE International Conference on Communications*. IEEE, 3670–3675.
- [2] Mahmuda Akter, Debjyoti Sengupta, Anurag Satpathy, and Sajal K Das. 2024. MIME: Mobility-Induced Dynamic Matching for Partial Offloading in Vehicular Edge Computing. In *2024 IEEE 49th Conference on Local Computer Networks (LCN)*. IEEE, 1–9.
- [3] Jorge Alcalde-Unzu and Elena Molis. 2011. Exchange of indivisible goods and indifferences: The top trading absorbing sets mechanisms. *Games and Economic Behavior* 73, 1 (2011), 1–16.
- [4] Mohammed Algafri, Anas Alghazi, Yasser Almoghathawi, Haitham Saleh, and Khaled Al-Shareef. 2024. Smart City Charging Station allocation for electric vehicles using analytic hierarchy process and multiobjective goal-programming. *Applied Energy* 372 (2024), 123775. doi:10.1016/j.apenergy.2024.123775
- [5] Bahram Alinia, Mohammad H Hajiesmaili, and Noël Crespi. 2019. Online EV charging scheduling with on-arrival commitment. *IEEE Transactions on Intelligent Transportation Systems* 20, 12 (2019), 4524–4537.
- [6] Peyman Ashkrof, Farnoud Ghasemi, Rafal Kucharski, Gonçalo Homem de Almeida Correia, Oded Cats, and Bart van Arem. 2025. The implications of drivers' ride acceptance decisions on the operations of ride-sourcing platforms. *Transportation Research Part A: Policy and Practice* 192 (2025), 104362.
- [7] Jørgen Bang-Jensen and Gregory Z Gutin. 2008. *Digraphs: theory, algorithms and applications*. Springer Science & Business Media.
- [8] Péter Biró, Flip Klijn, and Szilvia Pápai. 2022. Serial rules in a multi-unit Shapley-Scarf market. *Games and Economic Behavior* 136 (2022), 428–453.
- [9] Duncan Black et al. 1958. The theory of committees and elections. (1958).
- [10] Punyasha Chatterjee, Pratham Majumder, and Sajal K Das. 2025. V2VDisCS: Vehicle to Vehicle Distributed Charge Sharing in Intelligent Transportation Systems. *IEEE Transactions on Intelligent Transportation Systems* (2025).
- [11] Long Chen, Yunqing Zhang, Bin Tian, Yunfeng Ai, Dongpu Cao, and Fei-Yue Wang. 2022. Parallel driving OS: A ubiquitous operating system for autonomous driving in CPSS. *IEEE Transactions on Intelligent Vehicles* 7, 4 (2022), 886–895.
- [12] Zheyi Chen, Sijin Huang, Geyong Min, Zhaolong Ning, Jie Li, and Yan Zhang. 2025. Mobility-aware seamless service migration and resource allocation in multi-edge IoT systems. *IEEE Transactions on Mobile Computing* (2025).
- [13] Hwei-Ming Chung, Sabita Maharjan, Yan Zhang, and Frank Eliassen. 2020. Intelligent charging management of electric vehicles considering dynamic user behavior and renewable energy: A stochastic game approach. *IEEE Transactions on Intelligent Transportation Systems* 22, 12 (2020), 7760–7771.
- [14] Mehmet Hazar Cintuglu, Osama A Mohammed, Kemal Akkaya, and A Selcuk Ulugac. 2016. A survey on smart grid cyber-physical system testbeds. *IEEE Communications Surveys & Tutorials* 19, 1 (2016), 446–464.
- [15] Shadi Djavadian, Raymond G Hoogendoorn, Bart Van Arerm, and Joseph YJ Chow. 2014. Empirical evaluation of drivers' route choice behavioral responses to social navigation. *Transportation research record* 2423, 1 (2014), 52–60.
- [16] David Gale. 1974. The trade imbalance story. *Journal of International Economics* 4, 2 (1974), 119–137.
- [17] David Gale and Lloyd S Shapley. 1962. College admissions and the stability of marriage. *The American mathematical monthly* 69, 1 (1962), 9–15.
- [18] Xiaoliang Guang, Yuhuai Peng, and Chenlu Wang. 2025. Game-Based Multi-UAV Dynamic Collaborative with Energy-Efficient Hierarchical Information Sharing for Mobile Crowdsensing. *IEEE Transactions on Mobile Computing* (2025).
- [19] Rustamjan Hakimov and Onur Kesten. 2018. The equitable top trading cycles mechanism for school choice. *International Economic Review* 59, 4 (2018), 2219–2258.
- [20] RJ Hanowski, BH Kantowitz, and SC Kantowitz. 1998. *The Effects of Inaccurate Traffic Information on Driver Behavior and Acceptance of an Advanced In-Vehicle Traveler Information System*. Technical Report. United States. Department of Transportation. Federal Highway Administration
- [21] Shixuan Hou, Jie Gao, and Chun Wang. 2022. Optimization framework for crowd-sourced delivery services with the consideration of shippers' acceptance uncertainties. *IEEE Transactions on Intelligent Transportation Systems* 24, 1 (2022), 684–693.
- [22] Liang Hu, Jing Dong, and Zhenhong Lin. 2019. Modeling charging behavior of battery electric vehicle drivers: A cumulative prospect theory based approach. *Transportation Research Part C: Emerging Technologies* 102 (2019), 474–489.
- [23] Su Hu, Feifei Zou, Yinhao Xiao, Haiyang Ke, and Jin Wang. 2025. Integrating Embedded Cyber-Physical Systems in Smart Energy for AI-Enhanced Real-Time Crowd Monitoring and Threat Detection. *IEEE Transactions on Consumer Electronics* (2025).
- [24] IoTLab02. 2025. react-TTC. <https://github.com/IoTLab02/react-TTC.git>. GitHub repository.
- [25] Muhammad Irfan, Tayyab Tahir, Shujuan Huang, Sara Deilami, and Binesh Puthen Veettil. 2025. Optimizing Residential Energy Costs: A Novel Machine Learning Approach for Solar PV and EV Integration through Heuristic Price Signal Dispatch. *IEEE Transactions on Industry Applications* (2025).
- [26] Yanjie Ji, Weihong Guo, Phil Blythe, Dounan Tang, and Wei Wang. 2014. Understanding drivers' perspective on parking guidance information. *IET Intelligent Transport Systems* 8, 4 (2014), 398–406.
- [27] Donald B Johnson. 1975. Finding all the elementary circuits of a directed graph. *SIAM J. Comput.* 4, 1 (1975), 77–84.
- [28] Yahya Kabiri-Renani, Ali Arjomandi-Nezhad, Mahmud Fotuhi-Firuzabad, and Mohammad Shahidehpour. 2024. Transaction-Based Day-Ahead Electric Vehicles Charging Scheduling. *IEEE Transactions on Transportation Electrification* 10, 4 (2024), 8235–8245. doi:10.1109/TTE.2023.3348490
- [29] Daniel Kahneman and Amos Tversky. 2013. Prospect theory: An analysis of decision under risk. In *Handbook of the fundamentals of financial decision making: Part I*. World Scientific, 99–127.
- [30] Takehiro Kawasaki, Ryoji Wada, Taiki Todo, and Makoto Yokoo. 2021. Mechanism design for housing markets over social networks. In *Proceedings of the 20th international conference on autonomous agents and multiagent systems*. 692–700.
- [31] Kasper Kerkman, Theo Arentze, Aloys Borgers, and Astrid Kemperman. 2012. Car drivers' compliance with route advice and willingness to choose socially desirable routes. *Transportation research record* 2322, 1 (2012), 102–109.
- [32] Arindam Khanda, Anurag Satpathy, Amit Jha, and Sajal K Das. 2025. CARGO: A Co-Optimization Framework for EV Charging and Routing in Goods Delivery Logistics. In *2025 IEEE 50th Conference on Local Computer Networks (LCN)*. IEEE, 1–9.
- [33] Arindam Khanda, Anurag Satpathy, Anusha Vangala, and Sajal K Das. 2025. SMEVCA: Stable Matching-based EV Charging Assignment in Subscription-Based Models. In *Proceedings of the 26th International Conference on Distributed Computing and Networking*. 46–55.
- [34] Parisa Khoshdel, Saeid Abrishami, Mehdi Feizi, and Faeze Ramezani. 2025. CG-TTC: A coalitional game-based approach for resource sharing in a peer-to-peer cloud federation market. *Future Generation Computer Systems* (2025), 108016.
- [35] Jack S Levy. 1992. An introduction to prospect theory. *Political psychology* (1992), 171–186.
- [36] Huamin Li and Tian Tang. 2025. Deconstruction of Intelligent Vehicle Cyber-Physical System Based on Fuzzy Soft Set and Multi-Attribute Group Decision Making. *IEEE Transactions on Intelligent Transportation Systems* (2025).
- [37] Jiayan Liu, Gang Lin, Sunhua Huang, Yang Zhou, Christian Rehtanz, and Yong Li. 2022. Collaborative EV routing and charging scheduling with power distribution and traffic networks interaction. *IEEE Transactions on Power Systems* 37, 5 (2022), 3923–3936.
- [38] Xize Liu, Jingxu Chen, Xuewu Chen, and Xinlian Yu. 2025. Spatial spillover effects of shared micro-mobility on public transit in medium-sized cities. *Transportation Research Part D: Transport and Environment* 147 (2025), 104923.
- [39] Xiaoying Liu, Biao Zhou, Xianzhong Tian, Weihua Gong, and Kechen Zheng. 2025. Energy Consumption Minimization for Delay-sensitive Data Collection in UAVs-assisted WSN. *IEEE Sensors Journal* (2025).
- [40] Thayer Morrill. 2015. Making just school assignments. *Games and Economic Behavior* 92 (2015), 18–27.
- [41] Thayer Morrill and Alvin E Roth. 2024. Top trading cycles. *Journal of Mathematical Economics* 112 (2024), 102984.
- [42] Zeinab Nezami, Emmanouil Chaniotakis, and Evangelos Pournaras. 2025. When computing follows vehicles: Decentralized mobility-aware resource allocation for edge-to-cloud continuum. *IEEE Internet of Things Journal* (2025).
- [43] Long Pan, Enjian Yao, and Don MacKenzie. 2019. Modeling EV charging choice considering risk attitudes and attribute non-attendance. *Transportation Research Part C: Emerging Technologies* 102 (2019), 60–72.
- [44] Sina Parhizi, Amin Khodaei, and Mohammad Shahidehpour. 2016. Market-based versus price-based microgrid optimal scheduling. *IEEE Transactions on Smart Grid* 9, 2 (2016), 615–623.
- [45] Jianlei Qian, Kun Wang, and Napat Harnpornchai. 2025. Smart Platform for Matching and Optimizing Barter Using Artificial Intelligence and Blockchain. *Sensors and Materials* 37, 10 (2025), 4499–4518.
- [46] Nancy Stephens and Kevin P Gwinner. 1998. Why don't some people complain? A cognitive-emotive process model of consumer complaint behavior. *Journal of the Academy of Marketing science* 26, 3 (1998), 172–189.
- [47] Chittaranjan Swain, Manmath Narayan Sahoo, Anurag Satpathy, Sambit Bakshi, and Soumya K Ghosh. 2024. M-dafto: Multi-stage deferred acceptance based

fair task offloading in iot-fog systems. *IEEE Transactions on Services Computing* (2024).

[48] Chittaranjan Swain, Manmath Narayan Sahoo, Anurag Satpathy, Khan Muhammad, Sambit Bakshi, and Joel JPC Rodrigues. 2023. A-DAFTO: Artificial cap deferred acceptance-based fair task offloading in complex IoT-fog networks. *IEEE Transactions on Consumer Electronics* 69, 4 (2023), 914–926.

[49] Yuanjie Tu, Moein Khaloei, Nazmul Arefin Khan, and Don MacKenzie. 2024. Effect of trip attributes on ridehailing driver trip request acceptance. *arXiv preprint arXiv:2402.01650* (2024).

[50] Lee V White, Emma Aisbett, and Christa Shen. 2024. Time-varying rates prompt different responses as a function of home energy efficiency. *Energy and Buildings* 319 (2024), 114549.

[51] Yi-De Wu, Ming-Feng Ge, Zhi-Wei Liu, Wen-Yi Zhang, and Wei Wei. 2021. Distributed CPS-based secondary control of microgrids with optimal power allocation and limited communication. *IEEE Transactions on Smart Grid* 13, 1 (2021), 82–95.

[52] Hao Xiong and Jiadong Yu. 2025. Adaptive AI in Smart Grid: A Continual Reinforcement Learning Framework for Cyber-Physical Systems. In *ICC 2025–IEEE International Conference on Communications*. IEEE, 6197–6202.

[53] Bo You, Ludwig Dierks, Taiki Todo, Minming Li, and Makoto Yokoo. 2022. Strategy-proof house allocation with existing tenants over social networks. In *Proceedings of the 21st International Conference on Autonomous Agents and Multiagent Systems*. 1446–1454.

[54] Bo Yu, Shan Bao, Zeyang Li, Eric Rask, Henry X Liu, Jim Sayer, et al. 2022. Modeling drivers' route choices and route compliance when interacting with an eco-routing navigation system. (2022).

[55] Min Zhang, Frank Eliassen, Amir Taherkordi, Hans-Arno Jacobsen, Yushuai Li, and Yan Zhang. 2025. Self-Determination Theory and Deep Reinforcement Learning for Personalized Energy Trading in Smart Grid. *IEEE Transactions on Systems, Man, and Cybernetics: Systems* (2025).

[56] Jin Zhao and Qixia Dong. 2020. Allocation algorithm of CPS communication resources based on cooperative game. *Computer communications* 160 (2020), 63–70.

[57] Zubin Zheng, Shengcai Liu, and Yew-Soon Ong. 2024. Hybrid Memetic Search for Electric Vehicle Routing with Time Windows, Simultaneous Pickup-Delivery, and Partial Recharges. *arXiv preprint arXiv:2410.19580* (2024).